High-Temperature Slow Relaxation of the Magnetization in Ni_{10} Magnetic Molecules

S. Carretta,[1] P. Santini,[1] G. Amoretti,[1] M. Affronte,[2] A. Candini,[2] A. Ghirri,[2] I. S. Tidmarsh,[3] R. H. Laye,[3] R. Shaw,[3] and E. J. L. McInnes[3]

[1]*Dipartimento di Fisica, Università di Parma, I-43100 Parma, Italy*

[2] *CNR-INFM-S3 NRC and Dipartimento di Fisica, Università di Modena e Reggio Emilia, I-41100 Modena, Italy*

[3]*Department of Chemistry, University of Manchester, Manchester M13 9PL, United Kingdom*

(Received 25 May 2006; published 13 November 2006)

We investigate a family of molecular crystals containing noninteracting Ni_{10} magnetic molecules. We find slow relaxation of the magnetization below a temperature as high as 17 K and we show that this behavior is not associated with an anisotropy energy barrier. Ni_{10} has a characteristic magnetic energy spectrum structured in dense bands, the lowest of which makes the crystal opaque to phonons of energy below about 1 meV. We ascribe the nonequilibrium behavior to the resulting resonant trapping of these low-energy phonons. Trapping breaks up spin relaxation paths leading to a novel kind of slow magnetic dynamics which occurs in the lack of anisotropy, magnetic interactions and quenched disorder.

DOI: 10.1103/PhysRevLett.97.207201 PACS numbers: 75.50.Xx, 75.60.Jk, 76.60.Es

One of the most debated issues in the physics of magnetic molecules is how the spin dynamics are affected by interactions of spins with other degrees of freedom, in particular, nuclear spins and phonons [1–5]. These interactions induce decoherence of the spin dynamics, usually leading to relaxation of molecular observables to their thermal-equilibrium value. The comprehension of these relaxation mechanisms in crystals containing magnetic molecules is not only an intriguing issue of fundamental interest, but it is also of critical importance for the envisaged technological applications of these molecules as classical or quantum bits. For temperature $T \gtrsim 1$ K, relaxation is due to spin-phonon interactions, with phonons behaving as heat bath and inducing thermalization by irreversible exchange of energy with spins. When T is increased, relaxation times drop because phonon populations $n_{\rm ph}$ rise very rapidly. The class of molecules retaining macroscopic times at the highest T ($\lesssim 3$ K) is that of molecular nanomagnets [1–3], where the reversal of the magnetization M is hampered by a uniaxial anisotropy energy barrier. Other mechanisms potentially leading to blocking of M are intermolecular exchange interactions or, at very low T ($\lesssim 1$ K), phonon bottleneck due to the smallness of the lattice heat capacity.

In this Letter, we focus on a family of molecular crystals, containing *noninteracting* magnetic Ni_{10} molecules, which we find to display slow relaxation of M below about 17 K in the lack of any anisotropy barrier. Thus, Ni_{10} is not a molecular nanomagnet: the high-T nonequilibrium behavior is completely different from that observed in nanomagnets and cannot be explained within the above-outlined framework of phonon-assisted relaxation. The distinguishing feature of Ni_{10} is a magnetic spectrum with a dense bandlike group of states at low energy, well separated (by 14 meV) from all other levels. We propose that this causes an unprecedented form of resonant phonon trapping [6], and a resulting breakdown of the heat-bath assumption for phonons: phonon populations $n_{\rm ph}$ are not fixed solely by the thermostat temperature, but also result from the very slow joint dynamics of phonons and spins. The resulting cooperative many-time-scales magnetic dynamics partially recalls that of spin glasses, but here it is associated to neither interactions nor disorder.

In the Ni_{10} family of compounds, the magnetic core consists of 10 Ni^{2+} ions arranged on a supertetrahedron [Fig. 1(a) and [7,8]). Ni_{10} cores are well separated and embedded in crystalline-ordered molecular structures, where the molecular and crystal symmetries are dictated by the specific organic ligands used. The preparation and the structure of $[Ni_{10}(O)(thme)_4(dbm)_4(O_2CPh)_2(EtOH)_6]$ [''Ni_{10}(EtOH)''] have been reported previously [8].

The six Ni ions bisecting the edges of the supertetrahedon can be divided into three pairs, each pair of ions being connected by a linear Ni-O-Ni superexchange bridge passing through the center of the tetrahedron. This bridge yields a very strong antiferromagnetic (AF) interaction $J\mathbf{s}_a \cdot \mathbf{s}_b$ between the $s = 1$ spins of the two Ni ions in each pair. Other superexchange interaction constants are expected to be much weaker, in particular, the one (J') between these six Ni ions and the four Ni ions at the vertices. Therefore, we expect the six central Ni ions to be frozen in a nonmagnetic singlet state for $k_B T \ll J$, separated by a large gap of order J from excited states. The four vertex Ni ions are then coupled to each other only in second and higher order perturbation theory with respect to J'. Thus, the exchange energy spectrum consists of a series of bands of states of width $\mathcal{O}(J'^2/J)$ separated by large gaps of order J [7]. The lowest-energy band contains 19 total-spin multiplets for a total 81 levels, and its exchange structure is approximately described by an AF effective Hamiltonian

$$H_{\rm eff} = J_{\rm eff}/2 \sum_{i \neq j=1,4} \mathbf{s}_i \cdot \mathbf{s}_j \qquad (1)$$

with $J_{\rm eff} \propto J'^2/J$. The spectral structure sketched above is confirmed by fits of the T- and field-dependence of the dc

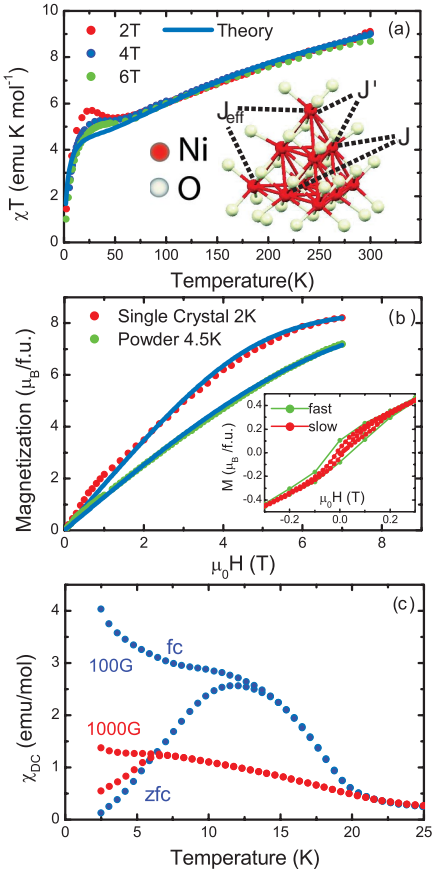

FIG. 1 (color). (a) Measured T- and H-dependence of $\chi_{\mathrm{dc}}T$ ($\chi_{\mathrm{dc}} = M/H$). The blue curved line is the theoretical fit assuming equilibrium. Inset: Molecular structure of Ni_{10}(EtOH). Ni-Ni bonds are guides to the eye. (b) Magnetization measurements performed at 2 K on single crystal (red circles) and at 4.5 K on powder sample (green). Absolute values were scaled with powder data. Inset: zoom view of the powder magnetization curve at 4 K. The hysteresis curve depends on preparation conditions (sweeping rate, powder or single-crystal). Here the green line is measured 10 times faster than the red line. (c) ZFC and FC susceptibility on powders. The procedure is the following: T is initially set to 40 K and H to zero. The sample is cooled at 2 K/min down to 2 K. At 2 K, H is switched on. ZFC measurements are taken by warming the sample up to 25 K, typically in ~1hr. FC measurements are taken by cooling down to 2 K at the same rate, keeping the field switched on.

magnetization M measured on powder and single-crystal samples (Fig. 1). By diagonalizing the full Hamiltonian of the 10 Ni spins, we find $J \simeq 14.6$ meV, $J' \simeq 1.1$ meV [7], and a Ni^{2+} gyromagnetic factor $g \simeq 2.25$. The spectrum contains a low-lying band of states well separated (by about 14 meV) from higher-lying states. Note that for small field H, $\chi_{\mathrm{dc}}T$ *vs* T displays a peak below ~20 K. In the next paragraph, we will show that for these fields and temperatures, Ni_{10} is not at equilibrium on the time scale used for this type of measurements. Hence, we have determined the Hamiltonian parameters by fitting only high-T and/or high-field magnetization data, for which preparation-dependence and nonlinearity tend to disappear. As far as magnetic anisotropy is concerned, we have made measurements on different single crystals and we have found *no angular dependence* of M within our experimental accuracy. The most important anisotropic contribution is the coupling of the four vertex $s = 1$ Ni^{2+} spins with the crystal field (CF) generated by their ligands. The local symmetry at the vertex sites is very low, with a first shell of ligands forming distorted octahedra. As usual, experimental information is by far insufficient to fix all local CF parameters, the only experimental constraint here being that the molecule does not display detectable uniaxial magnetic anisotropy (unlike in nanomagnets). A simple possible choice for the local CF is a coupling of the form $H_{\mathrm{CF}} = \sum_{i=1,4} d[s_{\zeta_i}^2 - s(s+1)/3]$, where s_{ζ_i} is the component of the spin of the ith vertex ion along the corresponding tetrahedron axis. For Ni^{2+} in distorted octahedral environment, the CF parameters have typically values of a few cm^{-1} [9]. Thus, we have fixed $d = -1\ \mathrm{cm}^{-1} \simeq -0.12$ meV. This CF has overall tetrahedral symmetry and produces only tiny dependence of $M(\mathbf{H})$ on the orientation of $\mathbf{H}$. We have checked that other choices for the sign and the value of d or other possible forms of H_{CF} lead to similar results. At last, the small intramolecular dipolar interaction is evaluated in the point-dipole approximation. The calculated lowest-energy band is shown in Fig. 2(a).

We now focus onto the low-T behavior of Ni_{10}. In Fig. 1(a), $\chi_{\mathrm{dc}}T$ shows a bump at ~20 K. In Ref. [8], this

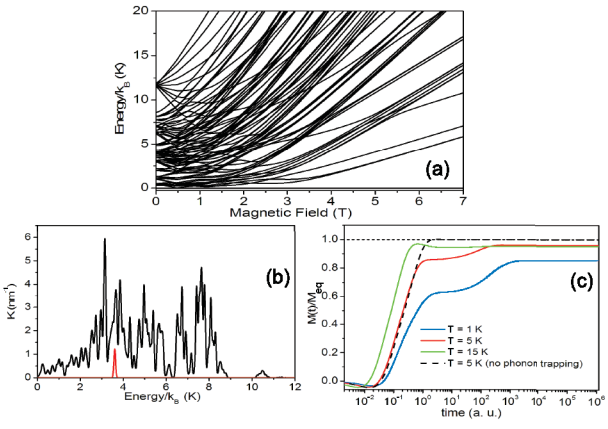

FIG. 2 (color). (a) Energy levels of the lowest-lying band as a function of H (oriented along one of the four tetrahedron axes). (b) High-T absorption coefficient $K(E)$, calculated as $K(E) = \sum_{s>t} W_{st}(N/V)P_{st}(E)/(81c\rho(E))$, where W_{st} are given by Eq. (2) with $\alpha = 10^{-4}\ \mathrm{THz}^{-2}$, $c = 3 \times 10^5$ cm/sec is the sound velocity, $\rho(E)$ is the phonon density of states (assumed Debye), and $P_{st}(E)$ is a line shape, assumed to be a Gaussian centered at $E_s - E_t$ with a standard deviation $\sigma/k_B = 0.04$ K ($H = 100$ G). Lorentzians yield an even denser spectrum. (c) Calculated time-dependence of M/M_{eq} (M_{eq} being the equilibrium value of M) for three representative temperatures (continuous lines) and $H = 100$ G. The dashed line represents $M(t)$ at 5 K calculated by neglecting phonon trapping. Initial conditions are equipopulation for magnetic levels and equilibrium occupations for phonons [7].

behavior had been tentatively ascribed to the appearance of long-range magnetic order. Yet, this looked odd since no intermolecular exchange pathway could be identified and $\chi_{dc}(T)$ displays no anomalies. By synthesizing and analyzing various Ni_{10} derivatives [7], we have now established that changing the ligands, and therefore the packing and distances between different molecules, leaves the susceptibility behavior almost unaffected. Moreover, we have also measured the specific heat of Ni_{10}(EtOH), and we find no anomalies in its T-dependence [7]. Thus, long-range magnetic order must be ruled out. Indeed, the low-T behavior is a nonequilibrium one. This is directly evidenced by the fact that the low-field magnetization M is markedly time- and history-dependent for $T \lesssim 17$ K. In particular, M exhibits different behavior if a zero field cooling (ZFC) or field cooling (FC) procedure is used. The ZFC curves lie below the FC one; with measurement rates of hundreds of minutes and $H = 100$ G, the opening of the ZFC and FC curves occurs at ~15 K close to the temperature of the maximum in the ZFC magnetization curve [Fig. 1(c)]. Furthermore, $M(H)$ at fixed T displays hysteretic behavior [Fig. 1(b)]. To clarify this point, we measured the time evolution of M using different preparation procedures. Some results are reported in Fig. 3(a) and 3(b). The typical relaxation behavior is multiexponential: a first fast decay (few seconds and less) followed by a second relaxation time scale of few minutes, a further decay on the time scale of a few hours, and finally a slow drift on the time scale of days or even longer. Starting from the ZFC curve, M increases with time, whereas it decreases when starting from the FC curve. In addition, the long-time value of M is significantly different for FC and ZFC protocols [7]. This means that the system does not relax to equilibrium within the experimental time scale, but rather it gets trapped in preparation-dependent out-of-equilibrium states. Remarkably, if Ni_{10} is field cooled in a magnetic field, when the field is switched off, a sizeable fraction of the magnetization M is retained for hours [Fig. 3(b)]. The ac susceptibility $\chi_{ac}(T, f)$ has been measured at different frequencies f. Both the in-phase χ'_{ac} and the out-of-phase component χ''_{ac} [Fig. 3(c) and 3(d)] abruptly increase below 20 K, and they show peaks at ~17.5 K, ~13 K, and ~8 K. We define a blocking temperature T_0 in correspondence of the first peak in χ'_{ac}. The temperature at which χ_{ac} peaks depends very weakly on frequency. This behavior is remarkably different from that of a nanomagnet and an unphysical value of the anisotropy barrier is obtained by assuming an activated Arrhenius mechanism. Moreover, there is evidence that Ni_{10} is still in a nonequilibrium long-living state up to $\sim 2T_0$. In fact, $M(H)$ is nonlinear even for tiny H [Fig. 3(b)], where any equilibrium model would predict perfect linearity since $\mu_B H/k_B T \ll 1$. However, this is not accompanied by relaxation on the time scale of few hours for $T > T_0$.

To summarize, Ni_{10} displays nonexponential relaxation with many time scales below T_0 and it is characterized by a nonlinear $M(H)$ up to $\sim 2T_0$. Since Ni_{10} has no anisotropy barrier, the observed long relaxation times cannot originate from the same phonon-assisted, barrier-crossing mechanism as in nanomagnets. Nevertheless, we have analyzed the relaxation properties of Ni_{10} in contact with the phonon heat bath. The main contribution to the magnetoelastic (ME) coupling comes from the modulation of the electric-quadrupole moment of each Ni ion by phonons [5], leading to transition rates W_{st} between levels t and s given by

$$W_{st} = \alpha \pi^2 \Delta_{st}^3 n_{\rm ph}(\Delta_{st}) \sum_{i,j=1,10} \sum_{q_1,q_2=x,y,z} \langle s|O_{q_1,q_2}(\mathbf{s}_i)|t\rangle \times \langle s|O_{q_1,q_2}(\mathbf{s}_j)|t\rangle^*, \quad (2)$$

where the first sum runs over Ni ions, $O_{q_1,q_2}(\mathbf{s}_i) = (s_{q1,i}s_{q2,i} + s_{q2,i}s_{q1,i})/2$ are quadrupolar operators, $n(x) = (e^{\hbar x/k_B T} - 1)^{-1}$, and $\Delta_{st} = (E_s - E_t)/\hbar$. Equation (2) is based on the simplest conceivable Debye model for phonons in which each Ni ion experiences a spherically symmetric ME coupling, but results do not depend qualitatively on this specific choice. The single free parameter α characterizes the coupling strength, and it is expected for Ni^{2+} to be of the order of 10^{-4} THz^{-2}. At $T = 5$ K, this yields relaxation times of less than about 10^{-8} sec, i.e., hugely shorter than the observed times.

In the preceding analysis, a crucial assumption is that phonons behave like a heat bath, establishing thermal contact with the thermostat instantaneously. This assumption requires that once a phonon is emitted by a molecule, it

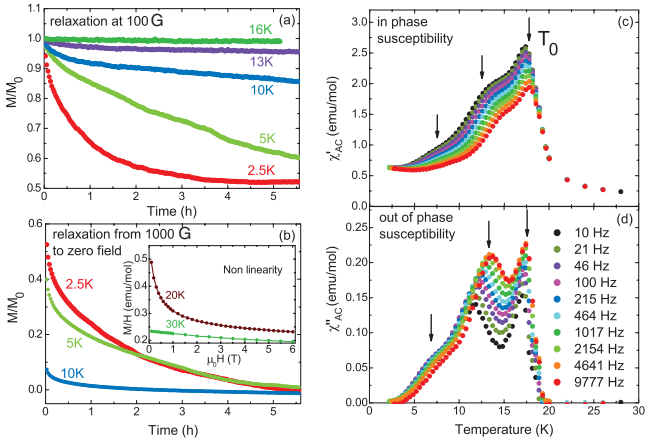

FIG. 3 (color). (a) Relaxation of M after preparation in FC conditions. A powder sample is cooled in a field of 100 G from 40 K at 2 K/min down to a fixed temperature $\tilde{T}$. When $\tilde{T}$ is reached, relaxation starts (time $t = 0$). $M_0 = 0.075$, 0.074, 0.059, 0.049, $0.034\mu_B$/f.u. from bottom to top. (b) Relaxation in the same condition as in (a), but the cooling is in 1000 G and the field is switched off as soon as $\tilde{T}$ is reached. $M_0 = 0.25$, 0.24, $0.2\mu_B$/f.u.. from top to bottom. Inset: M/H vs H, clearly showing the nonlinear behavior of M, even for T as high as 20 K or 30 K. In-phase (c) and out-of-phase (d) components of χ_{ac} measured on powder Ni_{10}(EtOH) with an ac field of 10 Oe at different frequencies. Data are taken on cooling, and a typical measurement from 30 K to 2 K lasts ~2 hrs.

is not further reabsorbed by other molecules. Reabsorption by nearby spins may lead to resonant trapping of the phonons involved in the relaxation process [6,10,11]. An intuitive picture [6] for an ensemble of 2-level systems is that a resonant phonon is continuously emitted and reabsorbed until it is emitted on the wing of the resonance line, where its free path is larger than the sample size L. We name $K(E)$ the absorption coefficient, i.e., the probability of phonon absorption per unit length. By defining the energy E_c such that $K(E_c)L = 1$, the trapping time τ in units of emission time T_1 will be approximately the ratio of the whole line intensity to the intensity beyond E_c. Magnetic molecules have generally well-separated energy levels, and are qualitatively similar to the above-mentioned 2-level systems. Therefore, we may generally expect effects on relaxation similar to those of 2-level systems, i.e., at very low T only.

Two features of Ni_{10} make it atypical: the first one is the presence of a dense band of low-lying levels. The second one is the highly nonaxial character of the anisotropy. As a result, the ME interaction, which is quite large for Ni^{2+}, can induce transitions between many pairs of levels, with gaps often close to each other on the scale of level widths (typically a few μeV [12]). Thus, the E-dependence of the absorption coefficient $K(E)$ is very different from that of a two-level system and recalls that of a band [Fig. 2(b)]. The red line in Fig. 2(b) represents a typical phonon emission spectrum corresponding to a given transition. By using the same rough line of reasoning as above, τ should be proportional to the ratio of the whole red line intensity to its intensity beyond $E_c/k_B \sim 9$ K. This number is clearly huge, implying that phonons with $E < E_c$ experience almost complete trapping, and the crystal is opaque to them [13]. As a result, the phonon populations $n_{\mathrm{ph}}(E)$ are not fixed to their thermal-equilibrium value as in Eq. (2), but evolve slowly in time jointly with spin populations. Modelling this dynamics is nontrivial even for the much simpler single-resonance, two-level systems [10,11]. Here, besides having thousands of involved resonances, there is the additional fundamental difficulty that since relaxation times are longer than the experimental window, initial conditions for populations depend in unknown way from the system history.

To grasp some essential features of the relaxation behavior of Ni_{10} in the trapped-phonon regime, we model it by a system of coupled master equations. These describe the joint evolution of the populations of the molecular magnetic levels of the lowest band $p_l(t)$ ($l = 1, 81$), and of the occupation numbers of Debye acoustical phonons $n_{\mathrm{ph}}(E, t)$ [7] (as in, e.g., [10]). The t-dependence of p_l and n_{ph} is calculated numerically. Some results are shown in Fig. 2(c). The model captures several key properties evidenced by experimental data. First of all, it displays virtually infinite relaxation times even for a degree of trapping much smaller than that expected from Fig. 2(b). At large times, the dynamics gets trapped in nonequilibrium states, as experimentally observed. The calculated time-dependence [Fig. 2(c)] is preparation-dependent and nonexponential, similarly to what was observed experimentally (Fig. 3). As T is increased, phonon trapping progressively gets less effective, and observables relax faster to nonequilibrium values closer to equilibrium ones. In addition, if the applied field intensity is increased, trapping is reduced because of the progressive opening of transparency windows in the phonon absorbance $K(E)$. This agrees, for example, with the lowering of the FC-ZFC splitting temperature, and with the fact that peaks in the ac susceptibility (Fig. 3) disappear when H is increased.

Our model only mimics the lowest-energy band of Ni_{10}, while real Ni_{10} has an additional energy scale, i.e., the gap (about 14 meV) separating ground- and first-excited bands. Thus, Ni_{10} can also relax by Orbach processes exploiting high-E phonons to bridge this gap. This induces an abrupt fastening of the relaxation dynamics [7] around 20 K, and we interpret the characteristic temperature scale T_0 as the one marking the onset of these interband processes.

In conclusion, Ni_{10} provides the first example of a novel kind of slow magnetic dynamics which occurs in the lack of magnetic interactions and anisotropy barriers. This high-T nonequilibrium behavior is completely different from that observed in molecular nanomagnets and cannot be explained within the conventional framework of phonon-assisted relaxation. We propose an unprecedented form of resonant phonon trapping to occur, leading to a breakdown of the heat-bath assumption for phonons. Similar slow dynamics, even at higher T, is expected to characterize molecular systems with analogous energy spectrum.

This work was carried out within the framework of the EC-Network of Excellence MAGMANet.

[1] R. Sessoli, *et al.*, Nature (London) **365**, 141 (1993).
[2] W. Wernsdorfer, *et al.*, Phys. Rev. Lett. **96**, 057208 (2006).
[3] D. Gatteschi and R. Sessoli, Angew. Chem., Int. Ed. **42**, 268 (2003).
[4] A. Fort *et al.*, Phys. Rev. Lett. **80**, 612 (1998).
[5] P. Santini *et al.*, Phys. Rev. Lett. **94**, 077203 (2005).
[6] P. W. Anderson, Phys. Rev. **114**, 1002 (1959).
[7] See EPAPS Document No. E-PRLTAO-97-007643 for additional figures and technical details. For more information on EPAPS, see http://www.aip.org/pubservs/epaps.html.
[8] R. Shaw *et al.*, Chem. Commun. (Cambridge) (2004) 1418.
[9] A. Abragam and B. Bleaney, *Electron Paramagnetic Resonance of Transition Ions* (Clarendon Press, Oxford, 1970).
[10] P. L. Scott and C. D. Jeffries, Phys. Rev. **127**, 32 (1962).
[11] D. L. Huber, Phys. Rev. **142**, 137 (1966).
[12] A. Mukhin *et al.*, Phys. Rev. B **63**, 214411 (2001).
[13] Spatial diffusion of the trapped phonons is neglected as the diffusion time to the thermostat is huge.